ISSN: 1415-7314
ISSN online: 2317-6717

ENGEVISTA
Página da revista: http://www.uff.br/engevista/seer/

Case study of magnetic fields in overhead transmission lines operating at steady state

Paula Carvalho Resende[1]

Gustavo Lobato Campos[2]

Mariana Guimarães dos Santos[3]

Abstract: Various equipment currently used emit high-intensity magnetic field, such as transmission lines, even operating at steady state. The magnetic fields generated by the transmission lines are influenced by the line configuration and voltage. Some studies have linked exposure to magnetic fields with the development of some diseases and interference in electronic equipment, so the study of such fields is crucial. The objective of this paper is to present algorithm developed in Matlab® to calculate the magnetic field in transmission lines operating at steady state. For this, it is discussed the magnetic field calculation methods commonly used to transmission lines. The algorithm is validated by means of comparison with other results of the literature and with results of measurement of two real lines of the Furnas system.

Keywords: Case study; magnetic field; Matlab®; transmission line.

[1] CEFET-MG – Centro Federal de Educação Tecnológica de Minas Gerais
[2] IFMG – Instituto Federal de Minas Gerais
[3] IFMG – Instituto Federal de Minas Gerais

Todos as informações e direitos sobre o presente artigo são de total e única responsabilidade do(s) autor(es).

ISSN: 1415-7314
ISSN online: 2317-6717

1. Introduction

Transmission lines are responsible for transporting the generated power to substations. Therefore, it is important to interconnect electrical system for economic dispatch of power during normal operation and emergency or power failure. Overhead transmission lines are composed of the support structures and associated equipment. Basic equipment is conductor cables, insulators, support structures already mentioned, and shielded wires. Transmission lines can operate in a steady state at frequencies of 50 - 60 Hz or transient state where frequencies reach up to 10 MHz (LAFOREST, 1981).

Thus, at end of the project of a transmission line is expected to achieve desired power transfer reliability and cost-effective, without causing environmental impacts and socioeconomic. To reduce ohmic losses, energy transmitted by transmission lines is made in high voltage. Despite high voltage, currents of the transmission lines are also high and induce a magnetic field around them (LAFOREST, 1981; SAWMA *et al*., 2010).

However, magnetic fields generated by transmission lines cause some concern in society due to a few associated problems. Some studies have linked exposure to magnetic fields with some pathologies affecting human health. In addition, magnetic fields may cause interfere communication network, interference in electrical and electronic devices, radio interference, and, audible noise. Another fact calls attention is difficult to access to the areas where transmission lines are installed to measure magnetic fields. Therefore, International Commission on Non-Ionizing Radiation Protection (ICNIRP) establishes that the maximum exposure limit for the general public is 200 μT (YU *et al*., 2016; CLAYTON, 2006; SANTOS, 2011; ICNIRP, 1998).

Thus, computer simulations to analyze magnetic fields present in different transmission lines configurations are tools that help and facilitate the verification of field levels to ensure security for the people and for the next installation of the transmission lines.

In the work reported here, we will develop and present magnetic field calculation methods mostly used in the literature for transmission lines operating at steady state. With these methods, will be developed a computational routine in Matlab®. The computational results will be compared with real magnetic field measurements to evaluate which method approaches the real measurement values.

2. Calculation methodology

Before presenting the mathematical models to calculate magnetic field it is necessary to establish some relevant premises of power transmission lines. In most electromagnetic modeling, there are physical and mathematical approximations.

Todos as informações e direitos sobre o presente artigo são de total e única responsabilidade do(s) autor(es).

ISSN: 1415-7314
ISSN online: 2317-6717

Therefore, overhead transmission lines in question will be considered three-phase, symmetrical and balanced. That is, the operating voltage has the same amplitude for the three phases and 120° lag and operates at steady state.

The current of a transmission line varies according to the power demand of the line users. Thus, the current used for the calculation is the average current of the transmission line. Current of the shielded wires is not considered in the calculations because they are small currents induced by phase cables.

In the next topics, it is presented the magnetic field calculation methods for transmission lines considering assumptions mentioned above. Specific considerations will be referred to and commented upon when necessary.

2.1 Ampère's Law

Ampere's Law defines in its integral form, showed in Equation (1) (SHADIKU, 2004), that line integral of the tangential component of magnetic field, $\vec{H}$ [A/m], around of a closed path is equal contour current, I_C [A], involved in this path.

$$\oint_C \vec{H} \bullet \overrightarrow{d\ell} = \int_S \overrightarrow{J_C} \bullet \overrightarrow{dS} = I_C \tag{1}$$

The conductive cables of a transmission line have a cylindrical shape. In addition, conductor cable length is in the order of kilometers, wherefore, it is possible to approximate the conductors with lengths that tend to infinity (SHADIKU, 2004).

Thus, for a cylindrical conductor of infinite length considering constant the vertical distance between the point of the field source and the observation point, ρ, Equation (1) can be reduced to Simplified method, describe in Equation (2) (SHADIKU, 2004).

$$\vec{H} = \frac{I}{2\pi\rho}\hat{a}_\phi \tag{2}$$

Which I [A] is the current flowing through the transmission line, $\hat{a}_\emptyset$ is the cross product between the current vector $\hat{a}_L$ and the position vector $\hat{a}_\rho$ as shown in Equation (3) which indicates the magnitude and orientation of the magnetic field at the observation point.

$$\hat{a}_\phi = \hat{a}_L \times \hat{a}_\rho \tag{3}$$

Todos as informações e direitos sobre o presente artigo são de total e única responsabilidade do(s) autor(es).

ISSN: 1415-7314
ISSN online: 2317-6717

Measurements and field analyses are performed on magnetic flux density $\vec{B}$, given in Tesla. Thus, Equation (4) (SHADIKU, 2004) determines the relationship between magnetic field $\vec{H}$ and magnetic flux density $\vec{B}$, which μ_0 is the magnetic permeability of vacuum.

$$\vec{B} = \mu_0 \vec{H} \tag{4}$$

Equation (2) is only valid for the magnetic field calculation generated by an immersed line in one environment, in this case, the air. However, the ground also has an influence on the magnetic field results and its inclusion is done by the Method of Images.

2.2 Method of images

Method of Images establishes that a current flowing above an environment considered a perfect conductor, $\sigma \rightarrow \infty$, induces a current in the opposite direction located symmetrically to its image in an environment considered perfect conductor (ZAHN, 1979). This method is used to represent the currents that penetrate in the ground, which influence in the magnetic field results at the observation point.

Therefore, considering conductor cables with infinite lengths, the magnetic flux density resulting in the observation point is the superposition of the magnetic fields generated by the real current and image current of each phase, represented in Equation (5) (ZAHN, 1979).

$$\vec{B}_T = \mu_0 \left(\sum_{I=1}^{N} \frac{I}{2\pi\rho_R} \hat{a}_{\phi R} + \sum_{I=1}^{N} \frac{I}{2\pi\rho_I} \hat{a}_{\phi I} \right) \tag{5}$$

Which the suffix “R” represents the components of the real currents, the suffix “I” represents the elements of the imaginary currents and, N represents the number of phase cables of the transmission line.

However, the ground has physical and electrical characteristics. Thus, the insertion of the ground effect in the magnetic field calculations would be more appropriate. There are several models where the ground effect is included. The Method of the Complex Ground Return Plane created by Deri *et al*. (1981) includes the ground effect by means of a complex ground return plane.

2.3 Method of the complex ground return plane

Method of the complex ground return plane consists of the design of a complex plane of return of current by the ground, with infinite conductivity and located below the ground at a

Todos as informações e direitos sobre o presente artigo são de total e única responsabilidade do(s) autor(es).

ISSN: 1415-7314
ISSN online: 2317-6717

distance equal to the complex penetration p (SANTIAGO & CUNHA, 2009). Equation (6) is the formulation proposed by Deri *et al*. (1981) for calculation of the complex depth p.

$$p = \frac{1}{\sqrt{j\omega\mu_0(\sigma_S + j\omega\varepsilon_S)}} \tag{6}$$

Which ω is the angular frequency in rad/s, μ_0 is the magnetic permeability of vacuum equal to $4\pi \times 10^{-7}$ H/m, σ_S is the ground conductivity in S/m and, ε_S is the ground electrical permittivity in F/m.

As mentioned in section 1, the magnetic field analyzes are done in steady state, 50 Hz - 60 Hz. Studies carried out by Vieira (2013) and Gertrudes (2005; 2010) for low frequencies, report that Equation (6) can be reduced to Equation (7). According to Vieira (2013) and Gertrudes (2005; 2010) the reduction of Equation (6) is physically consistent and practically does not influence the calculation of the longitudinal parameters of transmission lines.

$$p = \frac{1}{\sqrt{j\omega\mu_0\sigma_S}} = \sqrt{\frac{\rho_S}{j\omega\mu_0}} \tag{7}$$

Which ρ_S is the ground resistivity. Figure 1 illustrates the Method of the Complex Ground Return Plane for a single-phase system. It can be observed that the image current, in this method, considers the complex depth.

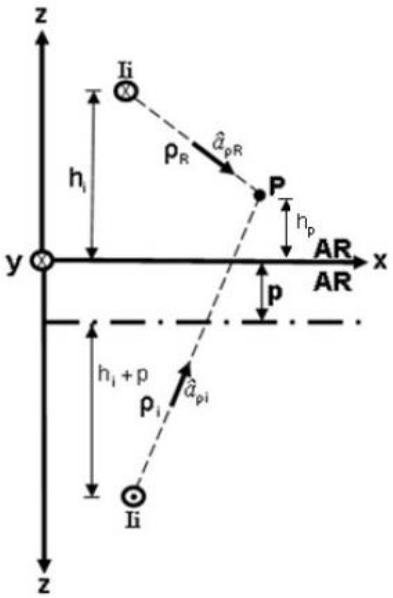

Figure 1: Method of the Complex Ground Return Plane for a single-phase system (VIEIRA, 2013).

Todos as informações e direitos sobre o presente artigo são de total e única responsabilidade do(s) autor(es).

ISSN: 1415-7314
ISSN online: 2317-6717

Thus, the final calculation of the magnetic flux density to the method of the complex ground return plane will only change the distances between the observation point and source field points, due to the insertion complex depth p. Equation (8) shows the final expression of the magnetic flux density.

$$\vec{B}_T = \mu_0 \left(\sum_{I=1}^{3} \frac{I_i}{2\pi(\rho_{Ri})^2} (h_p - h_i, 0, x_i - x_p) + \sum_{I=1}^{3} \frac{I_i}{2\pi(\rho_{Ii})^2} (-h_p - h_i, 0, x_p - x_i) \right) \quad (8)$$

Which I_i corresponds to the phase currents of each transmission line conductor, h_i is the height of the i-th conductor cable of i-th current, h_p is the height of the field observation point in relation to the ground, x_i and x_p are respectively the distances horizontal position of the i-th conductor cable and the observation point and, ρ_{Ri} and ρ_{Ii} are the vertical distances (real and image) between the field source point and the field observation point of the i-th conductor cable. All parameters can be observed in the Figure 1.

After the definition of the methods of calculation of magnetic field, it is developed a computational tool in Matlab® for the calculation of the magnetic fields generated by transmission lines. Then, to validate the algorithm, comparison is made of the obtained results and the literature results of the area, presented below.

3. Computational routine validation

When a computational tool is developed, it is crucial to confirm the accuracy and reliability of the results. For this, the results were compared with computational results and measurements of magnetic fields disseminate in the area literature.

The validation is presented by graphs and tables as a comparison of some important values, such as the maximum magnetic field value and its position. Will be presented a complete comparison, including the graphs, in order to exemplify how the results indicated in Tables 2 and 3 were achieved.

In 2013, Hugo Vieira (2013) conducted a study on the magnetic coupling between transmission lines and metal ducts. The author, Vieira (2013), uses three systems for computing the magnetic field. The structures of the transmission lines are shown in the Figure 2 and the electrical and geometric configurations are shown in the Table 1.

Todos as informações e direitos sobre o presente artigo são de total e única responsabilidade do(s) autor(es).

ISSN: 1415-7314
ISSN online: 2317-6717

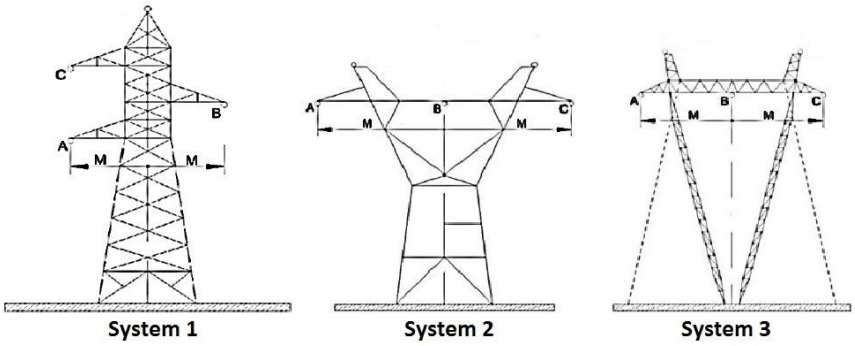

Figure 2: Structures of systems analyzed by Vieira (2013).

Table 1: Electrical and geometric characteristics of the systems analyzed by Vieira (2013).

System	Voltage	Current	Phase A	Phase B	Phase C	M
System 1	138 kV	146.43 A	12.15 m	14.01 m	15.87 m	3.00 m
System 2	345 kV	418.30 A	14.00 m	14.00 m	14.00 m	9.50 m
System 3	500 kV	837.15 A	16.53 m	16.53 m	16.53 m	10.25 m

Systems operating frequency is 60 Hz. The cross section is 60 m, 30 m on each side from the center of the structures. Field analysis is done at 1 m height. The ground resistivity considered by Vieira (2013) was 2400 Ω.m. Figure 3 and 4 shows the curves simulated by Vieira (2013) and the curves obtained from the computational routine as a result of this research for all the systems, respectively.

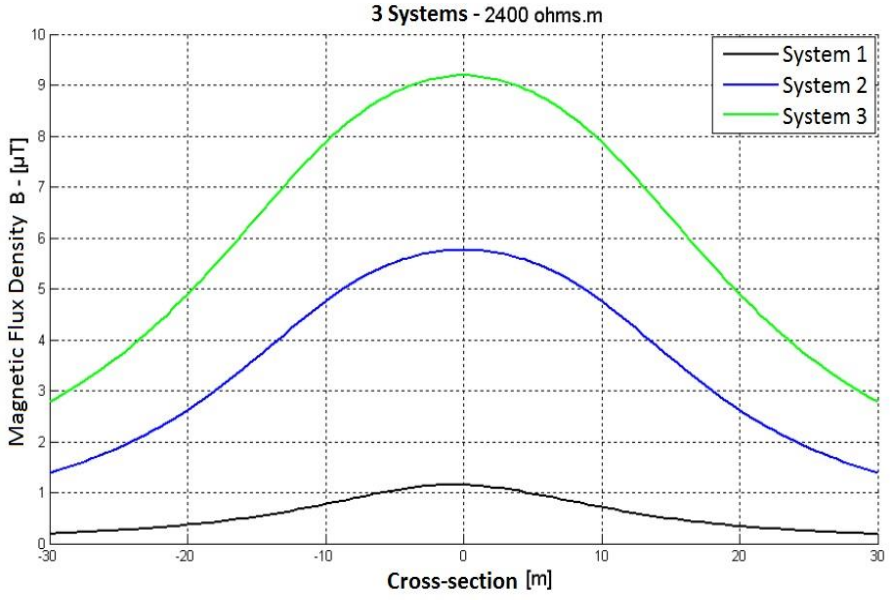

Figure 3: Magnetic field curves simulated by Vieira (2013).

Todos as informações e direitos sobre o presente artigo são de total e única responsabilidade do(s) autor(es).

ISSN: 1415-7314
ISSN online: 2317-6717

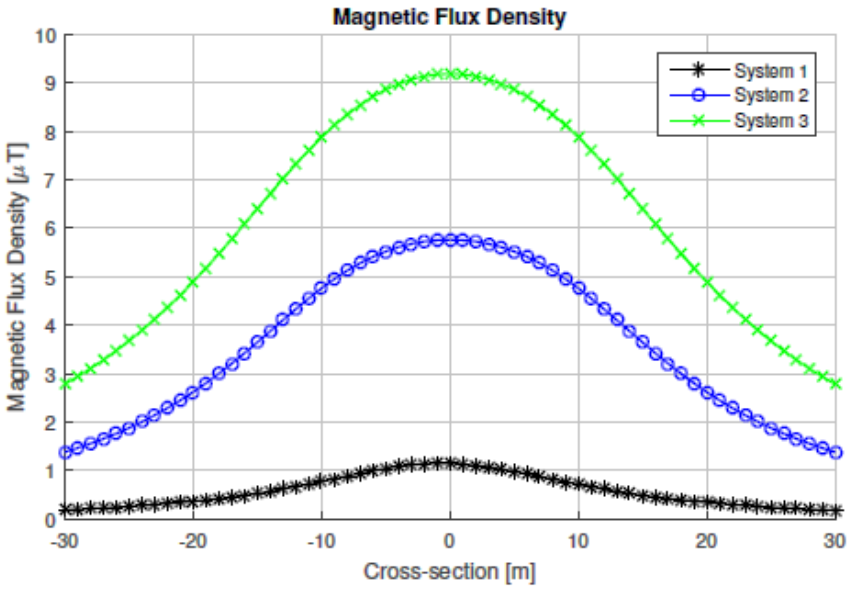

Figure 4: Magnetic fields curves obtained by Matlab® simulation.

The results obtained by the computational routine in Matlab® were also compared with computational results simulated by Nafar *et al.* (2013). To increase the algorithm reliability, it is compared the results with the values of measurements performed by Ramírez (2001) and Guimarães (2005) studies. The Tables 2 and 3 present the values of magnetic flux obtained by the authors, aforementioned, and the values obtained by the Matlab® algorithm. The values correspond to the magnetic field at the center of the transmission line, i.e., x=0.

A difference between the results simulated by the authors Nafar *et al.* (2013) and Vieira (2013) and the results obtained by the algorithm in Matlab® (Table 2) was extremely low. So, there was a huge similarity between field curves and ensures the reliability of the computational tool.

Table 2: Comparison between values simulated by Nafar *et al.* (2013) and Vieira (2013) and simulated values in this research.

Author		Voltage	Current	Authors S.	Matlab® S.	Error
Nafar *et al.* (2013)		63 kV	2000 A	8.30 µT	8.32 µT	0.24%
Vieira (2013)	Sys. 1	138 kV	146.43 A	1.14 µT	1.14 µT	0.00%
	Sys. 2	345 kV	418.43 A	5.76 µT	5.76 µT	0.00%
	Sys. 3	500 kV	837.15 A	9.18 µT	9.18 µT	0.00%

Todos as informações e direitos sobre o presente artigo são de total e única responsabilidade do(s) autor(es).

ISSN: 1415-7314
ISSN online: 2317-6717

Table 3: Comparison between the values measured by Ramírez (2001) and Guimarães (2005) and simulated in this research.

Author	Voltage	Current	Measurement	Matlab® S.	Error
Ramírez (2001)	230 kV	160 A	1.53 µT	1.37 µT	-10.00%
	500 kV	590 A	7.00 µT	8.11 µT	15.85%
Guimarães (2005)	500 kV	650 A	7.80 µT	8.24 µT	17.70%

However, the difference between the measurements presented by the authors Ramírez (2001) and Guimarães (2005) and the values simulated by the algorithm in Matlab® was slightly higher. This difference may occur due to factors such as current variation, temperature and air humidity that increase inaccuracy at the measurement time. However, measured and calculated magnitude magnetic field values are close, which is relevant for the computational tool validation and proves the mathematical formalism veracity.

4. Transmission lines under study – Estreito and Mascarenhas de Morais

The measurements data of two transmission lines were made available for study and analysis by the energy company Furnas from Brazil. Magnetic field measurements were performed on the Estreito (LTFUES) and Mascarenhas de Morais (LTFUMM) transmission lines. A transmission lines real photo is shown in Figure 5. Table 4 present the geometric and electrical characteristics of the LTFUES and LTFUMM lines, which D is the distance between the transmission lines and M the distance between the phases.

Todos as informações e direitos sobre o presente artigo são de total e única responsabilidade do(s) autor(es).

ISSN: 1415-7314
ISSN online: 2317-6717

Figure 5: Transmission lines - LTFUES and LTFUMM.

Table 4: Electrical and geometric characteristics of LTFUES and LTFUMM.

Characteristics	**LTFUES**	**LTFUMM**
Voltage	345 kV	345 KV
Current	309.5 A	293.8 A
Phase A	10.08 m	15.32 m
Phase B	10.45 m	15.45 m
Phase C	11.00 m	17.01 m
M	8.40	
D	32.00 m	

The cross-section considered in the measurement was 155 m, being 77 m for the LTFUES side and 78 m for the LTFUMM side. The symmetry axis is the center of the distance (D) between the transmission lines. The average current was considered for the computational simulations. The height of the instrument for the measurement was 1 m from the ground. The cross-section ground is irregular and therefore there are a difference in the phase cable heights.

Finally, a Figure 6 presents the magnetic field density values measured in 155 m cross-section between the transmission lines LTFUES and LTFUMM, considering the symmetry axis the center of the distance between the transmission lines. In topic 5, will be compared the measurement data of LTFUES and LTFUMM lines with the simulations of the magnetics models already presented in this paper.

Todos as informações e direitos sobre o presente artigo são de total e única responsabilidade do(s) autor(es).

ISSN: 1415-7314
ISSN online: 2317-6717

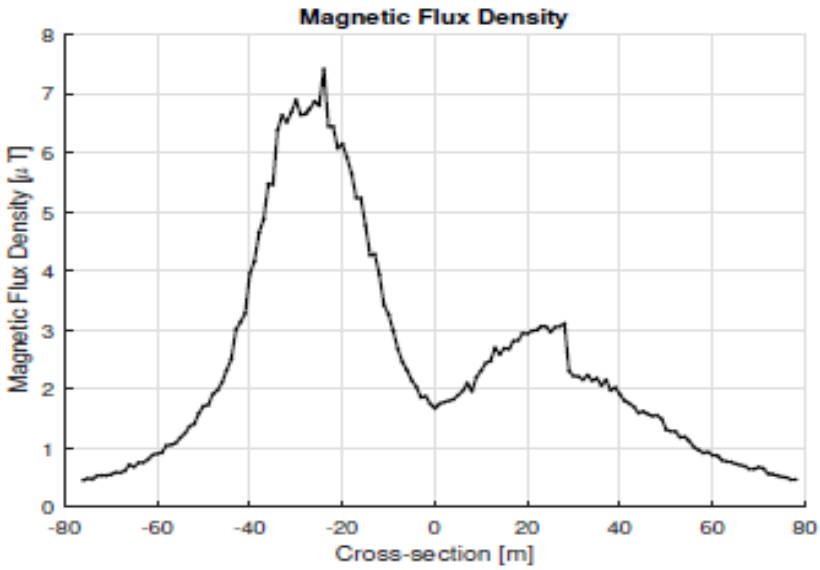

Figure 6: Measurement magnetic field curve.

5. Results and Remarks

5.1 Comparison of calculation methods with field measurements

Thus, with the proven validation of the computational tool, it is possible to compare the magnetic flux density measured values in the transmission lines under study with the computational values, analyzing each method described in topic 2.

Figure 7 shows the measured and simulated magnetic flux density curves in the Matlab® algorithm for each model of topic 2, considering the data in Table 4. In the simulations, the cross-section was 155 m, the field analysis height was 1 m, and the ground resistivity used was 2400 Ω.m.

Todos as informações e direitos sobre o presente artigo são de total e única responsabilidade do(s) autor(es).

ISSN: 1415-7314
ISSN online: 2317-6717

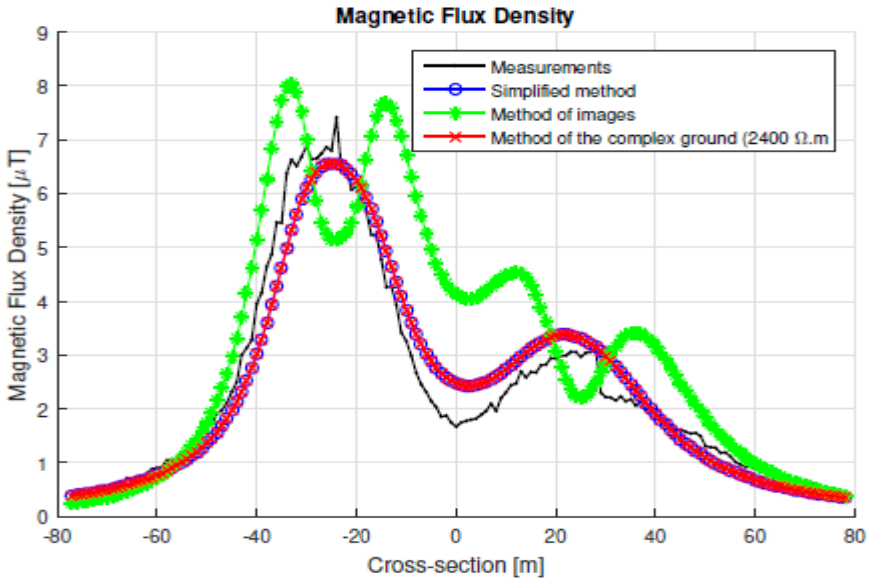

Figure 7: Measurement magnetic field curve and calculation methods curves.

Looking at Figure 7, some observations can be made:

- No magnetic field value exceeded the values established by ICNIRP mentioned in the section 1.
- The behavior of the measurement curve (black), the simplified method curve (blue) and, method of the complex ground return plane curve (red) are similar and the method of the complex ground return plane curve overlays the simplified method curve. The behavior of the magnetic field for the method of image is different and changes the maximum field points.
- There is interference between the generated magnetic fields. At the ends, the fields rapidly decrease to relatively low values, but between the transmission lines, this fact does not happen, due to the interference between them with the overlapping of the fields.
- The behavior of the measurement curve, simplified method curve and, method of the complex ground return plane curve was similar, but the absolute values had a small difference. There are several factors that can influence measurement values. The transmission line current depends on network energy demand. Thus, at the time of measurement, the current value may differ from the average current values used in the simulations. The air humidity and temperature can also influence the final value of the magnetic field.

Table 5 presents the errors between the measured and simulated values of each method. Case 1 is the error between measurement and simplified method. Case 2 is the error between the

Todos as informações e direitos sobre o presente artigo são de total e única responsabilidade do(s) autor(es).

ISSN: 1415-7314
ISSN online: 2317-6717

measurement and the method of images. Case 3 is the error between the measurement and method of the complex ground return plane.

Table 5: Error between measured values and calculation methods.

Position (m)	Case 1	Case 2	Case 3
0	48.50%	146.76%	48.50%
-76	-12.38%	-44.46%	-12.38%
77	-22.12%	-12.36%	-22.12%
-25	-3.38%	-24.15%	-3.38%
22	13.04%	-15.05%	13.04%

We can observe that the values vary greatly in case 2 since the method of images curve behavior are different. However, case 1 and 3 showed low variation proving the validity of the algorithm to calculate the magnetic field in a transmission line.

Analyzing Table 5, we observe that the cases 1 and 3 values were the same. However, the method of the complex ground return plane considers the ground effect in its calculations and the simplified method does not. Thus, subsection below, we will evaluate the ground influence in the magnetic field calculation.

5.2 Sensitivity field analysis in relation to ground resistivity

The method of the complex ground return plane uses in its calculations the ground effect, considering the resistivity $\neq 0$, being the correct mode of insertion of ground in the calculations, since the ground has its own characteristics.

To understand how the magnetic field behaves in relation to ground resistivity, we vary the ground resistivity in the method of the complex ground return plane simulations for transmission lines under study. Therefore, Figure 8 shows the magnetic field curves of the LTFUES and LTFUMM lines as a function of several resistivity values.

Todos as informações e direitos sobre o presente artigo são de total e única responsabilidade do(s) autor(es).

ISSN: 1415-7314
ISSN online: 2317-6717

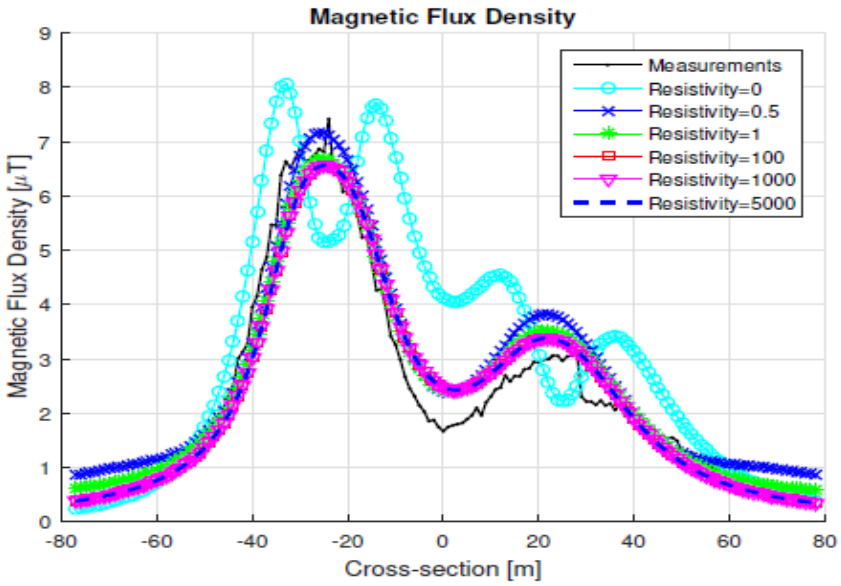

Figure 8: Magnetic field curves varying resistivity.

The measurement curve and the curves for resistivity values above 0.5 Ω.m show the same behavior. For resistivity values greater than 1 Ω.m, the magnetic field curves overlap and have equal maximum values. However, considering the ideal ground (resistivity = 0) the behavior of the curve modifies and the maximum field points are in different positions. Therefore, the method of the complex ground return plane tends to reduce the number of magnetic field maximum points when compared to the method of images. This fact happens due to the positioning of the image currents, which in the method of the complex ground return plane are positioned at higher distances in relation to the image currents of the ground with infinite conductivity.

According to studies carried out by Modema & Sueta (2011), there are no typical values of resistivity below 1 Ω.m. Therefore, regardless of the installation site of the transmission line, the ground will not influence the magnetic field calculations for low frequencies and can be calculated by the simplified method. Table 5 confirms this statement since the values of case 1 and case 3 were the same.

6. Conclusions

This paper aims to build a computational tool developed in Matlab® to calculate and analyze the magnetic field generated by two real transmission lines. In the magnetic field modeling, the ground effect was included, since its resistivity is different from zero. This fact increases the reliability of the results.

Todos as informações e direitos sobre o presente artigo são de total e única responsabilidade do(s) autor(es).

ISSN: 1415-7314
ISSN online: 2317-6717

To validate the computational calculations, we compared its results with results disseminated in the area literature. There was a great similarity in the results, confirming the computational tool validation.

Thus, measurements of transmission lines under study were compared with the modeling calculations presented in topic 2. We conclude that behavior with a magnetic field is sensitive to modeling. The behavior of the curve changes when the ground is considered the perfect electric conductor. However, for the calculation that does not consider the ground effect and the calculation that considers the characteristics of the ground, the behavior of the curves was similar. Thus, we conclude that the ground does not influence the magnetic field final value at low frequencies.

In summary, the Matlab® algorithm developed in this work proved to be reliable and versatile, since we can analyze any geometry and characteristics of a transmission line, with the minimum of final results errors.

7. References

CLAYTON, P. R. 2006. *Introduction Electromagnetic Compatibility*, Hoboken, Wiley-Interscience.

DERI, A., TEVAN, G., SEMLYEN, A. & CASTANHEIRA, A. 1981. The Complex Ground Return Plane a Simplified Model for Homogeneous and Multi-Layer Earth Return, *IEEE Transactions on Power Apparatus and Systems*, vol PAS-100, nº 8.

GERTRUDES, J. B. 2005. *Comportamento eletromagnético do solo no domínio da frequência: Tratamento de dados de campo e influência no desempenho de linhas aéreas de transmissão de energia.* Master thesis, Universidade Estadual de Campinas.

GERTRUDES, J. B. 2010. *Influência da condutividade e permissividade do solo em função da frequência do cálculo da impedância longitudinal e admitância transversal de linhas aéreas de transmissão.* Doctoral thesis, Universidade Estadual de Campinas.

GUIMARÃES, G. E. 2005. *Medições e cálculos de campos elétricos e magnéticos de uma linha de transmissão de 500 kV*. Master thesis, Universidade Federal de Minas Gerais.

ICNIRP - International Commission on Non-Ionizing Radiation Protection 1998. Guidelines for limiting exposure to time-varying electric, magnetic, and electromagnetic fields (up to 300 GHz), *Health Phys 74*, vol. 4, 494-522.

LAFOREST, J. J. 1981. *Transmission Line Reference Book – 345 kV and Above,* New York, United States General Electric Company.

MODEMA, J. & SUETA H. 2011. Medição da resistividade do solo, *O Setor Elétrico*, São Paulo, vol. 6, nº 70, 30-35.

Todos as informações e direitos sobre o presente artigo são de total e única responsabilidade do(s) autor(es).

ISSN: 1415-7314
ISSN online: 2317-6717

NAFAR, M., SOLOOKINEJAD, G. & JABBARI, M. 2013. Magnetic field calculation of 63 kV transmission lines, *International Journal of Research and Reviews in Applied Sciences*, nº 17, vol. 2.

RAMIREZ, J. A. Campos eletromagnéticos devido a sistemas de energia elétrica, Anais: Efeitos Biológicos Devidos à Ação de Campos Eletromagnéticos, 2001, São Paulo.

SANTIAGO, D. M. C. & CUNHA, R. C. Ferramenta computacional para cálculos de impedâncias características, funções de propagação e impedâncias de sequências de linhas de transmissão aéreas trifásicas, considerando os efeitos dos cabos para-raios do solo. 17ª Edição do Prêmio de Ciência e Tecnologia da Sociedade Mineira de Engenheiros (SME), 2009, Belo Horizonte.

SANTOS, M. G. 2011. *Acoplamento elétrico entre linhas de transmissão operando em regime permanente e dutos metálicos aéreos*, Master thesis, Universidade Federal de São João Del-Rei.

SAWMA, E., ZEITOUN, B., HARMOUCHE, N., GEORGES, S., HAMAD, M. & SLAOUI, F. H. Electromagnetic induction in pipelines due to overhead high voltage power lines. IEEE International Conference on Power System Technology, 2010, Zhejiang, China. 1-6.

SHADIKU M. N. O. 2004. *Elementos de eletromagnetismo*, Porto Alegre, Bookman.

VIEIRA, H. R. 2013. *Acoplamento magnético entre linhas de transmissão operando em regime permanente e dutos metálicos aéreos*. Master thesis, Universidade Federal de São João Del-Rei.

YU, Z., FU, Y., ZENG, R., TIAN, F., LI, M., LIU, L., LI, R. & GAO, Z. Data analysis of electromagnetic environment of UHVDC transmission lines. 12th IET International Conference on AC and DC Power Transmission, 2016, Beijing, China. 1-4.

ZAHN M. L. 1979. *Electromagnetic field theory: A problem solving approach*, New York, Wiley.

Todos as informações e direitos sobre o presente artigo são de total e única responsabilidade do(s) autor(es).